

The Formation of Nano-Dot and Nano-Ring Structures in Colloidal Monolayer Lithography[†]

J. Boneberg,* F. Burmeister, C. Schäfle, and P. Leiderer

Universität Konstanz, D-78434 Konstanz, Germany

D. Reim, A. Fery, and S. Herminghaus

MPI für Grenzflächenforschung, Rudower Chaussee 5, D-12489 Berlin Adlershof, Germany

Received May 12, 1997. In Final Form: October 8, 1997[®]

Monolayers of colloidal particles formed in a self-organizing process upon drying of a colloidal suspension are used as lithographic masks. After deposition of a thin metal layer, the mask is detached from the surface. The resulting surface is examined with optical, scanning electron, and atomic force microscopes. In addition to the well-known triangular structures, which reflect the gaps in the hexagonal arrangement of the particles, we observed the following additional features: hillocks (nano-dots) found just below and nano-rings found around the original location of the particles. These features may develop during detachment (hillocks) and formation (rings) of the mask, respectively. Hillocks develop as a consequence of the adhesion of the particles on the surface, whereas rings are formed from organic residuals in the suspension. We show that these features can be used to fabricate fluorescent dye rings of submicron size.

Introduction

The formation of hexagonally ordered monolayers of colloidal particles from suspension of colloidal particles has been examined in detail.¹⁻⁴ Several years ago the possibility of lithography by the help of these monolayers was discussed.^{5,6} This technique, in which the monolayer is used as deposition or etching mask, allows production of regularly arranged structures of triangular features of almost arbitrary materials. The characteristic length scale can be varied by the use of a proper particle diameter, which is available from 50 nm to 30 μm . Because this technique is quite inexpensive and relatively easily reproduced, it has attracted attention in different types of experiments in which nanostructures play an important role. Nanostructures produced in this way were used, for example, as phonon diffraction gratings⁷ or as test samples for optical nearfield microscopy (SNOM).^{8,9} Single-domain magnetic structures have been fabricated as well.¹⁰ A requirement for the fabrication of these masks is a smooth and hydrophilic substrate. Recently, it has been shown that by applying an additional floating process these masks can be used on nonwetting or even on curved surfaces as well.¹¹ For some applications, however, it would be

appreciable to overcome the restriction of triangular structures, dictated by the triangular holes in the hexagonal arrangement of the particles. One approach towards this direction is the use of different forms of ion etching.¹² By such an additional treatment, ellipsoidal silver particles have been produced and their optical properties have been studied.¹³ Nevertheless, in terms of simplicity of the method, a flexible choice of the form of the nanostructures already during the production process would be favorable. One example of a ring formation has been reported in the literature,¹⁰ but the formation process itself was not studied in detail.

Here we report a systematic study of nontriangular features, hillocks and rings, which we have observed during our experiments with colloidal masks. To understand the origin of these structures, we performed experiments with colloidal monolayers under different conditions and observed the resulting structures with optical, scanning electron, and scanning force microscopy. After a description of the experimental setups and the preparation methods, we discuss the experiments that lead to triangular structures, hillocks, and rings.

Experimental Section

The monolayers of latex spheres were produced by a slow evaporation of a colloidal suspension on a substrate following the method introduced by Micheletto et al.¹⁴ As substrates we used glass slides, which were cleaned successively in mucaol (Merz GmbH, Frankfurt), acetone, ethanol, and millipore water in an ultrasonic bath. In one case, a 20-nm thin Pt-film on glass was used. The latex spheres [Bangs Laboratories, Inc.; polystyrene, diameter (d) = 842 nm; IDC polystyrene (PS), d = 3 μm and 300 nm] were dispersed in millipore water. A droplet with a particles/water volume fraction of ~ 0.5 vol% (depending on particle size) was deposited on the glass substrate and mounted in a closed box with temperature control similar to the system described by Micheletto et al.¹⁴ For the metallic substrate, 20 vol% ethanol was added to enhance spreading of the solution. The typical evaporation time was several hours, resulting in 2 cm^2 of ordered latex spheres with typical crystallite sizes of 50 μm^2 .

[†] This paper is dedicated to the memory of Dieter Reim who passed away in April 1997.

[®] Abstract published in *Advance ACS Abstracts*, December 1, 1997.

(1) Denkov, N. D.; Velez, O. D.; Kralchesky, P. A.; Ivanov, I. B.; Yoshimura, H.; Nagayama, K. *Langmuir* 1992, 8, 3183.

(2) Denkov, N. D.; Velez, O. D.; Kralchesky, P. A.; Ivanov, I. B.; Yoshimura, H.; Nagayama, K. *Nature* 1993, 361, 26.

(3) Dushkin, C. D.; Yoshimura, H.; Nagayama, K. *Chem. Phys. Lett.* 1993, 204 (5,6), 455.

(4) Kralchesky, P. A.; Nagayama, K. *Langmuir* 1994, 10, 23.

(5) Fischer, U. C.; Zangsheim, H. P. *J. Vac. Sci. Technol.* 1981, 19, 881.

(6) Deckmann, H. W.; Dunsmuir, J. H. *Appl. Phys. Lett.* 1982, 41, 377.

(7) Vu, P. D.; Olson, J. R.; Pohl, R. O. *Ann. Physik* 1995, 4, 9.

(8) Koglin, J.; Fischer, U. C.; Fuchs, H. *Phys. Rev. B* 1997, 55 (12), 7977.

(9) Hecht, B.; Pohl, D. W.; Heinzelmann, H.; Novotny, L. In *Photon and Local Probes*; Marti, O.; Möller, R., Eds.; NATO ASI Series E: Applied Sciences; Vol. 300, 1995.

(10) Winzer, M.; Kleiber, M.; Wiesendanger, R. *Appl. Phys. A* 1996, 63, 617.

(11) Burmeister, F.; Schäfle, C.; Matthes, T.; Böhmisch, M.; Boneberg, J.; Leiderer, P. *Langmuir* 1997, 13, 2983.

(12) Deckmann, J. H. W.; Dunsmuir, H. *J. Vac. Sci. Technol. B* 1993, 1, 1109.

(13) Buncick, M. C.; Warmack, R. J.; Ferrell, T. L. *J. Opt. Soc. Am. B* 1987, 4, 927.

(14) Micheletto, R.; Fukada, H.; Ohtsu, M. *Langmuir* 1995, 11, 3333.

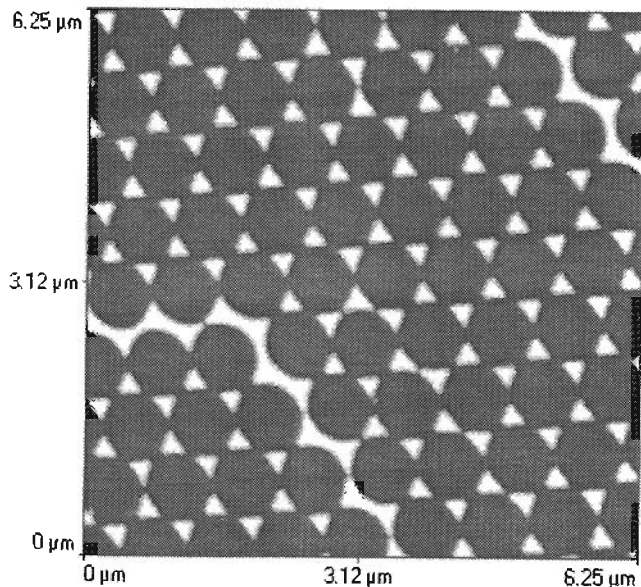


Figure 1. Topography (AFM contact mode, $6.25 \mu\text{m} \times 6.25 \mu\text{m}$) of a glass surface after deposition of 55-nm Au onto a monolayer of 842-nm particles and particle detachment. Triangular Au structures and Au wires can be observed.

For the deposition of the metal film, these masks were introduced in a high vacuum chamber. After evacuating to 1×10^{-6} mbar, a thin film of gold of several nanometers thickness was thermally deposited. Then the vacuum chamber was vented, and the latex spheres were removed by ultrasonic cleaning in millipore water. The remaining nanostructures were then analyzed by optical and scanning electron microscopy (SEM) as well as with different atomic force microscopes (AFM, two home-built AFMs and a Nanoscope III from Digital Instruments). One of these AFMs allows simultaneously topography and Kelvin-mode measurements where the local surface potential is measured (similar to the setup described by Weaver and Wickramasinghe¹⁵) with a lateral resolution of 20 nm and a resolution in the surface potential of 10 meV.

Results and Discussion

Triangular Structures. For a comparison with later results, Figure 1 shows the topography (measured by AFM in contact mode) of a glass surface after deposition of 55 nm Au onto the colloid monolayer ($d = 842$ nm) and successive detachment of the latex spheres in an ultrasonic bath. The hexagonal arrangement of the triangular structures can clearly be seen. Upon drying of the monolayers, the PS particles are shrinking, which leads to the formation of cracks. Therefore, 'metallic wires' can also be found on the surface. As expected, both triangles and wires have the height of the deposited Au film, which was 55 nm in this case. Triangles of this kind have been observed by different authors^{5-11,13} and will therefore not be discussed further.

Hillocks. Sometimes a different feature can be observed in these experiments. Figure 2 shows a SEM picture of an area where only the particles ($d = 842$ nm) on the left-hand side have been detached. The picture indicates round features in the region where the particles have been removed, which will hereafter be called hillocks. From a comparison with the location of the particles it can be concluded that these hillocks have been formed at the spots where the particles touched the surface. Because the contrast in SEM pictures cannot be directly related to topographic information, especially when different materials are involved, we also performed AFM measure-

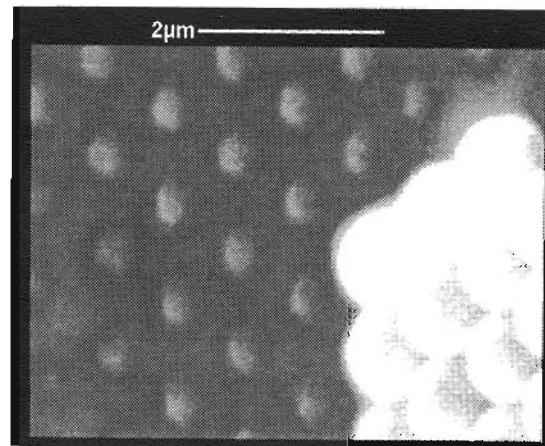


Figure 2. Electron microscope picture ($5.75 \mu\text{m} \times 4.2 \mu\text{m}$) of a surface with 842-nm particles. On the left-hand side, the particles have been detached and hillocks can be observed.

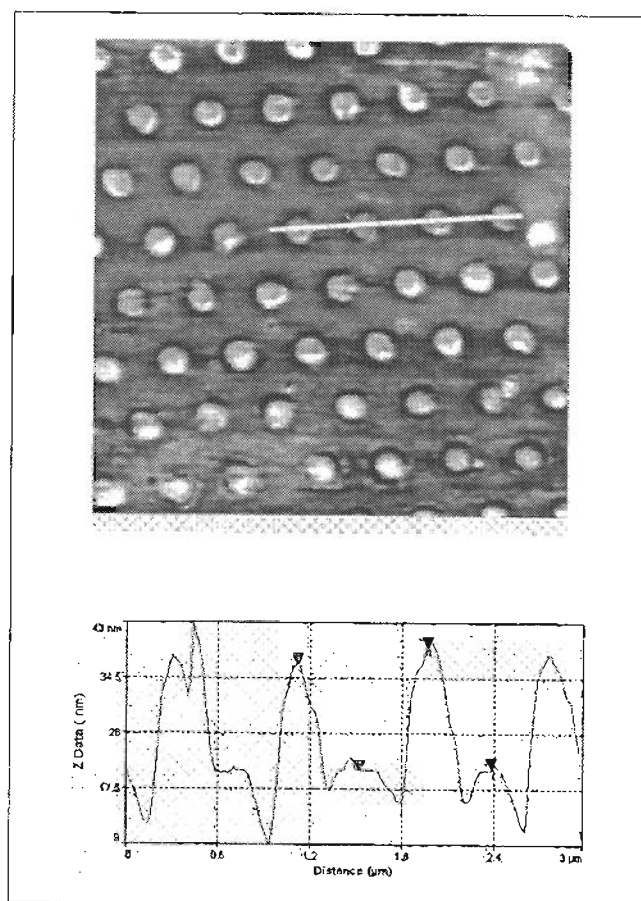


Figure 3. Topography (AFM contact mode, $5.7 \mu\text{m} \times 5.7 \mu\text{m}$) of hillocks on a surface similar to the left-hand part of Figure 2. The cross section is depicted for the indicated line.

ments. An AFM topography (contact mode) of a sample prepared in the same way (Figure 3) confirms the impression that these structures are elevated. Typical dimensions of the hillocks in that case are 300 nm in diameter and 40 nm in height.

We believe that these hillocks are formed as a consequence of the adhesion of the particles. A schematic picture is given in Figure 4. During formation of the monolayer, capillary forces deform the particles, whereby the contact area is enlarged.¹⁶ This sequence could be observed by electron microscopy (not shown here). As the

(15) Weaver, J. M.; Wickramasinghe, H. K. *J. Vac. Sci. Tech. B* 1991, 9, 1562.

(16) Dahneke, B. J. *Colloid Interface Sci.* 1972, 40, 1.

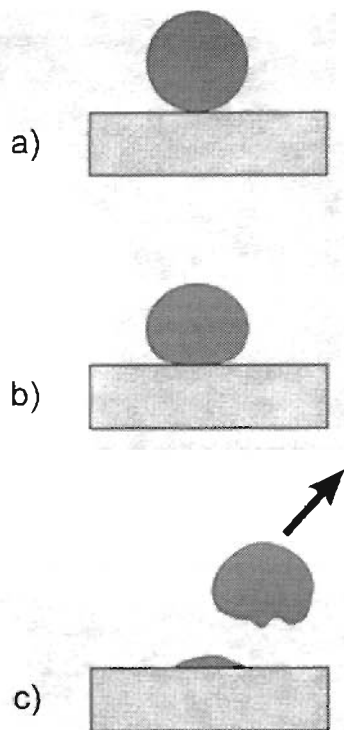


Figure 4. Schematic model for the formation of hillocks. (a) Shape of the particle in solution; (b) shape of the particle after complete drying of the solution; and (c) detachment of the particle.

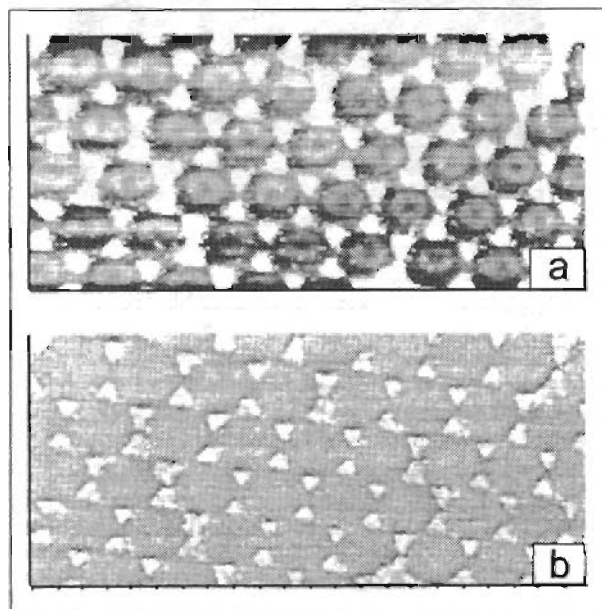


Figure 5. (a) Topography (AFM non contact mode, $6.75 \mu\text{m} \times 3.75 \mu\text{m}$) and (b) Kelvin mode signal of a sample with triangular structures and rings. The rings can not be observed in the Kelvin mode signal.

particles are detached, they may be torn if the internal fracture energy is smaller than the adhesion energy. Whereas the typical fracture energies of polystyrene particles¹⁷ are known to be in the range $15\text{--}230 \mu\text{J}/\text{m}^2$, adhesion energies are hard to predict because they may depend on, for examples, contact area, humidity, electrostatic attraction, polymer bridging, thin layers, and

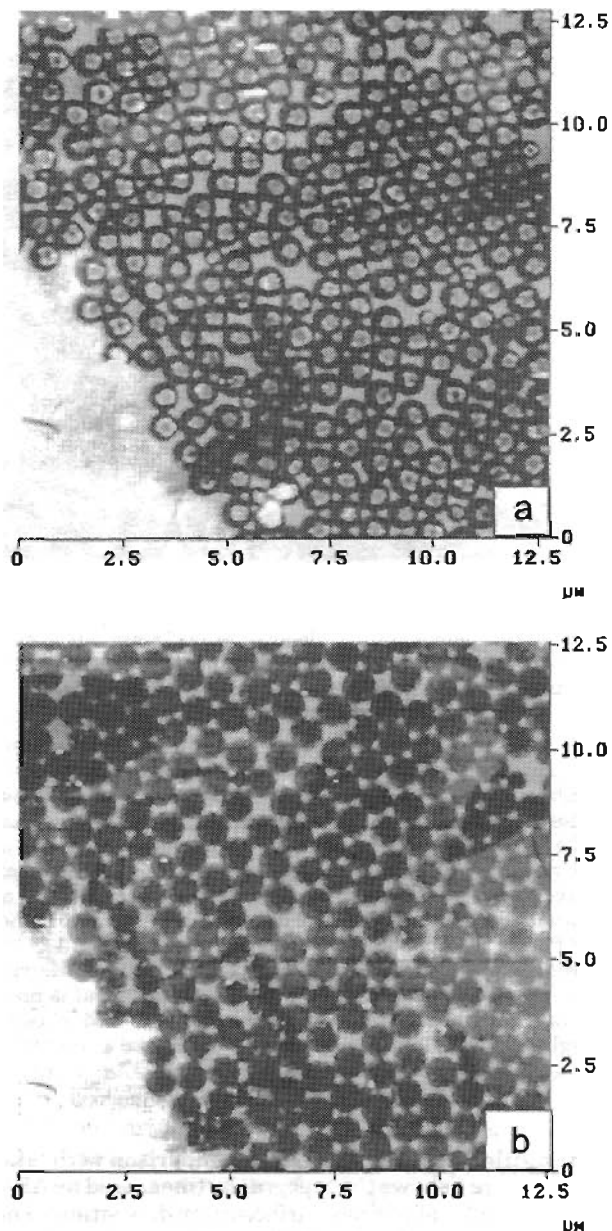


Figure 6. Topography (AFM noncontact mode, $12.5 \mu\text{m} \times 12.5 \mu\text{m}$) of a surface with triangular structures and rings before (a) and after treatment (b) with Caro's acid. The rings disappeared during the chemical treatment.

the chemical nature of the surface.^{18,19} In particular, the last point may be responsible for the experimental observation that hillocks never have been found to appear homogeneously over a sample. Although this model describes the experimental observations, for a complete understanding of the hillock formation process it would be necessary to perform further measurements with different surface preparations (e.g., surfaces consisting of areas with different surface potentials). This task seems to be difficult on a first glance because the formation of well-ordered monolayers requires a chemically homogeneous surface.¹⁻⁴ However, we have recently shown that this restriction can be circumvented by fabricating the monolayers on a glass substrate first and then transferring them to an arbitrary surface.¹¹

Rings. Figure 5 shows the result of an experiment where once again Au (60 nm) was deposited onto a

(17) Sambasivam, M.; Klein, A.; Sperling, L. H. In *Film Formation in Waterborne Coatings*; Provdor, T.; Winnik, M.; Urban, M., Eds.; ACS Symposium Series 648, 1996.

(18) Granier, V.; Sartre, A. *Langmuir* 1995, 11, 2179.

(19) Surface and Colloid Science, Matijevic, E., Ed.; John Wiley & Sons: New York, 1978.

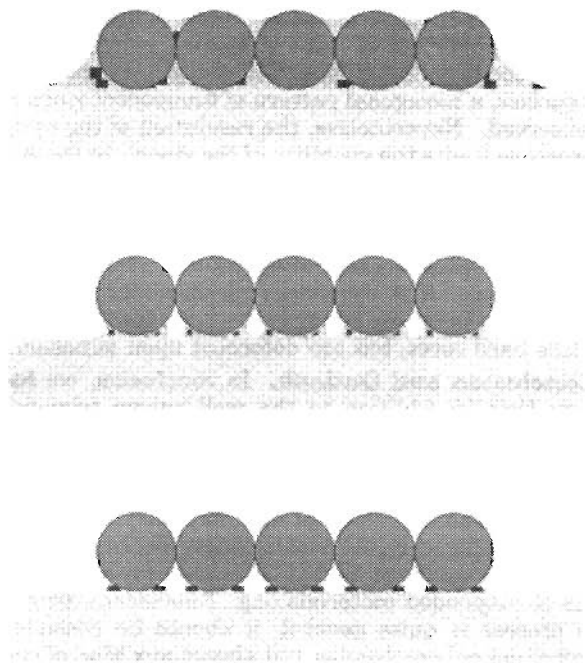


Figure 7. Schematic model for the formation of rings. During the evaporation of the liquid, micromenisci are formed around the contact area of the colloid particles with the surface. After complete drying, rings consisting of material dissolved in the suspension remain.

monolayer colloidal mask and the particles ($d = 842$ nm) were removed afterwards. In addition to the triangular structures, rings surrounding the original contact area of the particles can be observed now. Some of the samples showed rings only in some restricted areas of the surface. Nevertheless, compared with the hillocks, the chance to observe rings is distinctly higher. This formation of rings has been observed on different substrates; in the example shown here, the substrate was a 20-nm Pt-film on a glass plate. The metallic substrate was chosen to perform a Kelvin mode measurement on the same sample, where a conducting substrate is necessary. This technique detects the surface potential and therefore allows achievement of material contrast even in nanometer thin films.^{20,21} The result is shown in Figure 5b. Whereas the rings could be resolved in noncontact mode, they are not visible in the Kelvin mode. At the same time, the triangles show a contrast in contact potential of 50 mV compared with the Pt substrate (Figure 5b), which proves that the resolution of the Kelvin mode is high enough to distinguish between Au and Pt. From this measurement it can be concluded that the rings consist of a material different from the triangles.

For an even more stringent proof that the triangular structures and the rings consist of different materials, we performed a chemical test on a glass surface covered with both triangular Au structures and rings. The sample was exposed to Caro's acid²² (H_2SO_5 , peroxomonosulfuric acid), a strong oxidizing agent, for several hours. After removal from the acid, the substrates were rinsed in water and then dried in a stream of dry nitrogen. A comparison of the AFM images of the same area before and after the

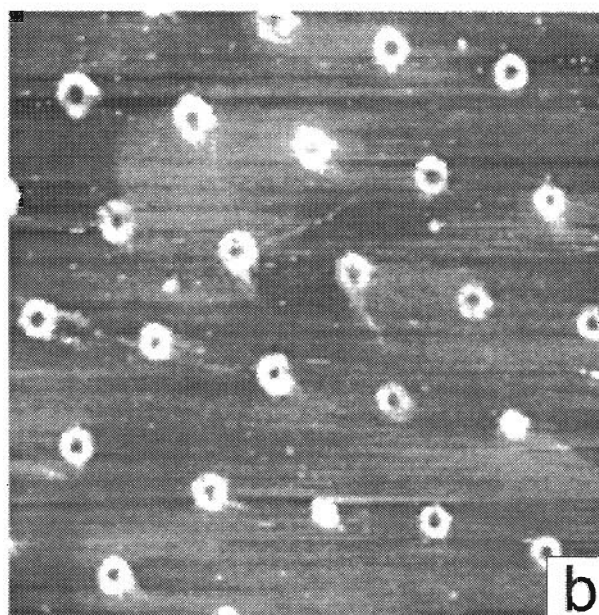
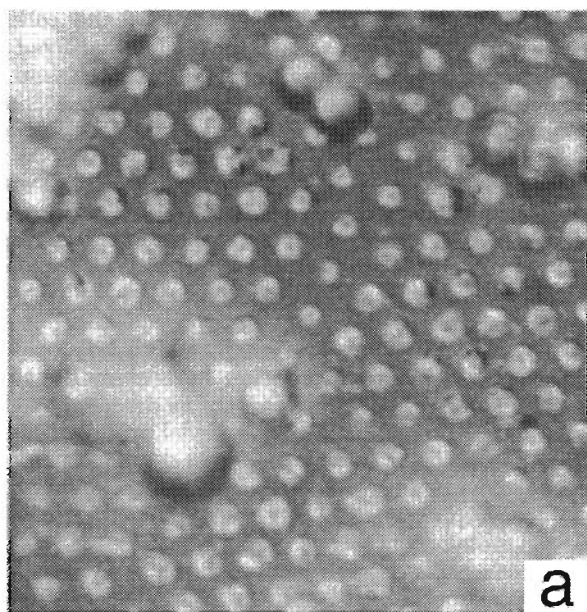


Figure 8. (a) Optical microscopy ($37.5 \mu\text{m} \times 37.5 \mu\text{m}$) and (b) AFM topography (contact mode, $15.4 \times 15.4 \mu\text{m}$) of a surface, where a droplet of rhodamin-6G was applied onto an already dried monolayer before the detachment of the particles. Fluorescent rings can be observed in the optical microscope. The AFM topography indicates a diameter of 600 nm.

treatment (Figures 6a and b) showed no effect of the chemical treatment on the Au and glass topography, whereas the rings completely disappeared. Thus it is clear that the rings are not made of the deposited metal. As this acid is especially used for removing organic residuals, this result suggests that the rings may consist of organic material and hence be formed already during the formation of the colloidal monolayer.

Our suggestion is further corroborated by a control experiment in which the colloidal monolayer was prepared on a glass surface and removed without any successive metal film deposition. Once again, rings could be found on the surface. This observation supports the following scenario for the formation of the rings (a schematic drawing is shown in Figure 7): As more and more liquid evaporates, capillary forces lead to the formation of

(20) Nonnenmacher, M.; O'Boyle, M.; Wickramasinghe, H. K. *Ultramicroscopy* **1992**, *42*, 268.

(21) Nonnenmacher, M.; O'Boyle, M.; Wickramasinghe, H. K. *Appl. Phys. Lett.* **1991**, *58*, 2921.

(22) Caro's acid was synthesized by adding potassium peroxodisulfate to sulfuric acid, which hydrolyzes via the following reaction: $\text{H}_2\text{SO}_5 \leftrightarrow \text{H}_2\text{SO}_4 + \text{H}_2\text{O}_2$. This scheme provides an almost constant, moderate concentration of peroxide, rendering it much less hazardous than the more generally used 'piranha solution'.

micromenisci around the contact area of the colloid particles with the surface. Polymer chains dissolved in the suspension are therefore forced to form rings around the colloidal particles. The observed polymeric residuals might consist of surfactants, which are added to most colloidal suspensions to stabilize the particles and prevent coagulation. This proposal is in complete agreement with the experimental result that we have never observed rings in surfactant-free suspensions up to now, whereas rings are frequently found after experiments with surfactant-containing suspensions. The interpretation is also supported by the surface potential measurement from Figure 6b, where no contrast between rings and Pt surface could be observed. We know from other measurements that even thick layers of polymers can not be detected by the Kelvin-mode.²³ In contrast to the model proposed here, the ring formation was explained by a diffusion process of deposited metal underneath the latex spheres by Winzer *et al.* Consequently, the rings should consist of the deposited metal. It might be possible that under certain circumstances this process occurs as well, but up to now it has not been observed in our experiments.

To prove the validity of our proposed model for the ring formation and to show a possible application we have applied a small droplet of rhodamin-6G dye dissolved in a mixture of methanol/water onto a monolayer of already dried 3- μm particles. The solution of these particles is surfactant free and, therefore, no rings could be observed as long as these colloids were used without the dye. Figure 8a shows a picture taken in an optical microscope. The particles were wiped off mechanically for this experiment,

(23) Steinke, R.; Hoffmann, M.; Böhmisch, M.; Eisenmenger, J.; Dransfeld, K.; Leiderer, P. *Appl. Phys. A* 1997, 64, 19.

so not all of them were removed. Some of the remaining particles appear out of focus of the optical microscope, because the focus is adjusted onto the glass surface. On the surface, a hexagonal pattern of fluorescent rings can be observed. Nevertheless, the resolution of the optical microscope limits the visibility of the rings. In the AFM topography (Figure 8b), rings with a diameter of 600 nm, a thickness of 150 nm, and a height of ~ 15 nm are resolved. In complete agreement with the proposed model, the dye molecules were arranged around the original contact area of the particle. The observed ring diameter of 600 nm once again reflects the fact that the 3- μm particles do not act like hard cores, but are deformed upon adhesion.

Conclusion and Outlook. In conclusion, we have shown that in addition to the well-known triangular structures, nano-dots and nano-rings can be found in colloid monolayer lithography. The dots are formed as a consequence of the adhesion of the colloids. The rings, on the other hand, develop through capillary forces from residual material in the suspension. We have demonstrated that this process can be used to fabricate nano-rings of suspended materials (e.g., fluorescent dye). As this process is quite general, it should be possible to arrange not only molecules, but almost any kind of small particles (e.g., metallic or semiconducting) into ring-like structures.

Acknowledgment. We thank M. Böhmisch and J. Zimmermann for the Kelvin-mode measurement, and C. Bechinger for stimulating discussion. Furthermore we are indebted to Dr. Roland Wagner for providing us with the formulation of Caro's acid used in this work.

LA9704922